Explicit Polarization (X-Pol) Potential Using ab Initio Molecular Orbital Theory and Density Functional Theory[†]

Lingchun Song,* Jaebeom Han, Yen-lin Lin, Wangshen Xie, and Jiali Gao*

Department of Chemistry, Digital Technology Center and Supercomputing Institute University of Minnesota, Minneapolis, Minnesota 55455-0431

The explicit polarization (X-Pol) method has been examined using ab initio molecular orbital theory and density functional theory. The X-Pol potential was designed to provide a novel theoretical framework for developing next-generation force fields for biomolecular simulations. Importantly, the X-Pol potential is a general method, which can be employed with any level of electronic structure theory. The present study illustrates the implementation of the X-Pol method using ab initio Hartree−Fock theory and hybrid density functional theory. The computational results are illustrated by considering a set of bimolecular complexes of small organic molecules and ions with water. The computed interaction energies and hydrogen bond geometries are in good accord with CCSD(T) calculations and B3LYP/aug-cc-pVDZ optimizations.

1. Introduction

Previously, we introduced an explicit polarization (X-Pol) method for condensed-phase and macromolecular simulations.[1−6] The X-Pol potential is based on electronic structure theory as a framework for developing next-generation force fields,[1−3] that is, to go beyond the traditional Lifson-type empirical potential (also known as molecular mechanics (MM))[7,8] used in essentially all current atomistic simulations of proteins and nucleic acids. The X-Pol potential is designed to make the fundamental paradigm change in the functional form of MM force field and in the representation of biomolecular systems. In the X-Pol method, a molecular system is partitioned into fragments, such as an individual solvent molecule or a peptide unit or a group of such entities. The electronic interaction within each fragment is treated using electronic structure theory, and the interactions between two fragments are described by Hartree product of the antisymmetric wave functions of individual fragments. Short-range exchange repulsion and long-range dispersion-like attraction between fragments are included by pairwise functions.[1−3] The variational X-Pol theory allows analytical gradients of the energy to be efficiently evaluated in dynamics simulations.[5] The X-Pol method is a general theory that can be implemented using any electronic structural methods including wave function theory (WFT) and density functional theory (DFT). Recently, we reported a molecular dynamics simulation of a fully solvated BPTI protein, consisting of 14 281 atoms and 29 026 basis functions,[6] employing the quantal X-Pol potential based on an approximate MO theory. It is possible to run about 3.5 ps (1 fs integration step) per day on a single 2.66 GHz processor.[6] That work demonstrated the feasibility of an entirely new concept in force field development for large-scale simulations. In this article, we illustrate the X-Pol method by making use of ab initio WFT MO theory and DFT, and present computational results on bimolecular interactions.

Before we begin, it is useful to briefly consider the past and current developments of molecular mechanical force fields, which date back to the pioneering studies of steric effects, independently by Hill[9] and by Westheimer,[10] and the subsequent developments of algorithms and applications to organic compounds.[11,12] The force field for biomolecular simulations was established by Lifson in the 1960s,[7,13] which led to the first molecular dynamics simulation of a protein by McCammon, Gelin, and Karplus.[14] Significant progress has been made in the accuracy of conventional force fields thanks to the tremendous efforts of parametrization by numerous groups in the past forty years. In fact, a major current push is to incorporate explicit polarization terms to treat electrostatic interactions.[15] Nevertheless, it is a sobering fact to note that the fundamental representation of biomolecular systems and the basic functional forms, including polarization terms,[16] in these force fields have hardly changed in the past forty years.[7,14,15,17,18] Undoubtedly, classical force fields will continue to be widely used and the accuracy will be further improved. However, despite the success of molecular mechanics in biomacromolecular modeling, there are also shortcomings, such as the arbitrariness in the choice of energy terms and the associated degrees of freedom, a lack of systematic approach to treat anharmonicity and cross coupling of energy terms, and the difficulty in describing electronic polarization and charge transfer. A fundamental change in force field development is warranted to increase the predictability of quantitative computational biology.

In the X-Pol potential, the system is treated explicitly by electronic structure theory and the wave function (or electron density) for each fragment is optimized by self-consistent field (SCF) method in the presence of the electric field due to all other fragments until the convergence is achieved for the entire system.[1−6] The internal energy terms and electrostatic potentials used in the classical force field are replaced and described explicitly by electronic structure theory. Consequently, they are obtained directly from quantum mechanical calculations, and electronic polarization and charge transfer are represented naturally in the theory. Furthermore, such a method can be directly used to model chemical reactions, electron transfer, and electronically excited states. The X-Pol potential, implemented using the semiempirical Austin Model 1 (AM1) method,[19] has been tested and applied to the simulation of liquid water[2] and

X-Pol Potential

J. Phys. Chem. A, Vol. 113, No. 43, 2009 **11657**

liquid hydrogen fluoride,[20] and has been extended to dynamics simulations of a fully solvated protein in aqueous solution.[6]

The X-Pol potential and its associated linear scaling method represent an entirely different approach from divide-and-conquer-type algorithms.[21–24] The divide-and-conquer (D&C)[21–24] and localized orbital methods[25] are linear scaling approaches to efficiently obtain a solution of the Hartree−Fock or Kohn−Sham equations for large molecular systems. In contrast, the X-Pol method is a quantum-mechanical force field (QMFF), whose energy is not the Hartree−Fock or Kohn−Sham DFT energy of the entire system.[1–6] Furthermore, the X-Pol potential is variational and can be efficiently used to carry out molecular dynamics simulations of solvated proteins,[5,6] whereas the D&C remains too time-consuming to carry out millions of electronic structure calculations for condensed-phase systems. The X-Pol potential also differs from combined quantum mechanical and molecular mechanical (QM/MM) approaches that employ a polarizable force field in the MM region.[26,27] The difficulties and uncertainties of treating molecular polarization in a classical force field are still present in coupled QM/MM-pol models. The mutual polarization of the entire system is treated consistently and equally in the X-Pol method.[1–3] Following our initial work,[1,2] Kitaura et al. described an approach, called fragment molecular orbital,[28,29] a procedure similar to the nonvariational, double self-consistent-field (DSCF) X-Pol method described in ref 1, and it has been successfully applied to numerous applications.[30] Recently, Gascon et al. published a self-consistent space-domain decomposition implementation of the X-Pol method for computing electrostatic potentials of proteins.[31] These authors used Morokuma's ONIOM scheme to carry out the DSCF optimization. Field also described a similar implementation making use of both the AM1 and HF/STO-3G method for water.[32] A closely related approach is the effective fragment potential (EFP) model developed by Gordon and co-workers.[33,34] The EFP method represents the electronic energies of interacting fragments by a set of analytical potentials optimized to fit the electronic structural data.

In what follows, we first present the X-Pol method with emphasis on the implementation using density functional theory. Then, in section 3, we describe the algorithm and computational details. Section 4 highlights the optimization strategies and results on bimolecular complexes. Finally, we summarize the major findings of this study and future perspectives on multilevel approaches for biomolecular modeling and simulations.

2. Theoretical Background

The X-Pol potential is based on a hierarchy of three levels of approximations.[1–5] At each level, if the approximation is not made, the X-Pol method reduces to the standard electronic structure theory at that stage. By applying these approximations, we achieve computational efficiency. Furthermore, it allows the introduction of one set of justifiable parameters associated with each approximation to achieve computational accuracy. For convenience of discussion, we consider a system of N closed-shell molecules, called fragments, that are not covalently connected. The generalization for treating covalently connected fragments has been described previously,[3] making use of the generalized hybrid orbital (GHO) scheme developed for combined QM/MM simulations.[35–39]

2.1. Level-1 (L1) Approximation and the Energy Expression of the X-Pol Potential. The first approximation in the X-Pol method is on the construction of the total molecular wave function, Φ (and the electron density), of the system, which is assumed to be a Hartree product of the antisymmetric wave functions of the individual fragments ($\{\Psi^A; A = 1,..., N\}$):[1]

$$\Phi = \prod_{A=1}^{N} \Psi^A \tag{1}$$

Here, the wave function Ψ^A may be approximated by a single determinant or by multiconfigurational methods such as the complete active space self-consistent field (CASCF) model or valence bond (VB) theory. In the rest of this article, the individual molecular wave function for fragment A is written as a single Slater determinant of m^A doubly occupied molecular orbitals, $\{\psi_i^A; i = 1,..., m^A\}$, which are linear combinations of atomic orbitals located on atoms of fragment A, subject to the orthonormal constraint:

$$\sum_{\mu\nu} c_{i\mu}^A c_{j\nu}^A S_{\mu\nu}^A - \delta_{ij} = 0 \tag{2}$$

where $c_{i\mu}^A$ and $c_{j\nu}^A$ are orbital coefficients and $S_{\mu\nu}^A$ is the overlap integral between atomic orbitals χ_μ^A and χ_ν^A in fragment A.

The approximation of eq 1 is equivalent to neglect of the exchange repulsion between electrons in different fragments, and the partition of the system into fragments ignores electron transfer and dispersion interactions.[1–3] However, this approximation is quite reasonable in the spirit of force field development and significantly simplifies computation. Nevertheless, it is essential to account for the energies due to exchange repulsion and dispersion attraction to prevent collapse of electrostatic interactions and to include van der Waals forces between different fragments, respectively, both of which are, in principle, dependent on the instantaneous molecular wave functions (or electron densities). An empirical or semiempirical approach based on perturbation theory is required to determine these energy terms,[1–3] for which one set of empirical parameters is introduced.

$$E_{int,ed} = \frac{1}{2} \sum_{A \neq B}^{N} E_{int,ed}^{AB}[\rho^A, \rho^B, \{\zeta^{AB}\}] \tag{3}$$

where ρ^A and ρ^B are the electron densities of fragments A and B, $E_{int,ed}^{AB}[\rho^A,\rho^B,\{\zeta^{AB}\}]$ specifies the exchange-repulsion and dispersion (ed) interaction functional of the two charge fragments, and $\{\zeta^{AB}\}$ is a set of atomistic parameters to correct the errors due to the Hartree-product approximation in eq 1.

The total energy of the system is given as follows:[1]

$$E_{tot} = \sum_{A=1}^{N} \left(E^A + \frac{1}{2} E_{int}^A \right) + E_{int,ed} \tag{4}$$

where E^A is the energy of fragment A with the wave function Ψ^A, E_{int}^A is the Coulomb interaction energy between fragment A and all other fragments, and $E_{int,ed}$ is the exchange-repulsion and dispersion energy among all fragments (see below).

In Hartree−Fock (HF) theory, the energy for fragment A, which is denoted by the subscript HF, is written as

$$E^A = E_{HF}^A = \sum_i 2H_i^A + 2\sum_{i,j} \left(J_{ij}^A - \frac{1}{2}K_{ij}^A \right) + E_{nuc}^A \tag{5}$$

where the subscripts i and j specify doubly occupied MOs in fragment A and the terms in eq 5 are respectively the one-electron integrals (H_i^A) that include the electronic kinetic energy and the electron−nucleus attraction, the Coulomb integrals (J_{ij}^A), the exchange integrals (K_{ij}^A), and the nuclear repulsion energy (E_{nuc}^A).

In DFT, the molecular orbitals, subject to the constraint of eq 2, are the Kohn−Sham (KS) orbitals,[40] from which the electron density for fragment A is obtained (this can readily be generalized to spin-polarized systems):

$$\rho^A(\mathbf{r}) = 2 \sum_i^{m^A} |\psi_i^A(\mathbf{r})|^2 \qquad (6)$$

The energy for fragment A is then

$$E^A = E_{DFT}^A[\rho^A(\mathbf{r})] = \sum_i 2H_i^A + \sum_{i,j} 2J_{ij}^A + E_{xc}^A[\rho^A(\mathbf{r})] + E_{nuc}^A \qquad (7)$$

where the first two terms have expressions identical to those in HF theory (eq 5), and the third term, $E_{xc}^A[\rho^A(\mathbf{r})]$, is the energy component accounting for all the effects of exchange and correlation of electrons in fragment A.

2.2. Level-2 (L2) Approximation and Coulomb Interactions between QM Fragments. The Coulomb interaction energy between fragment A and all other fragments arises from summations over electrons and nuclei from fragment A, and it has identical expressions for both DFT and HF theory:

$$E_{int}^A = \sum_i 2I_i^A + \sum_a L_a^A \qquad (8)$$

where a specifies an atom in fragment A. The two terms of eq 8, I_i^A and L_a^A, represent the interaction energies of orbital i and the nuclear charge of atom a of fragment A with the total external electrostatic potential (ESP) due to all other fragments in the system.[1,3] The external ESP on fragment A is given as follows:

$$V^A(\mathbf{r}) = \sum_{B \neq A} \left[-\int \frac{\rho^B(\mathbf{r}')}{|\mathbf{r} - \mathbf{r}'|} d\mathbf{r}' + \sum_b \frac{Z_b^B}{|\mathbf{r} - \mathbf{R}_b^B|} \right] \qquad (9)$$

where the summation is over all fragments except A, $\rho^B(\mathbf{r}')$ is the electron density of fragment B and $\mathbf{R}_b^B$ and Z_b^B are the nucleus position and charge of atom b in fragment B. Thus,

$$I_i^A = \langle \psi_i^A | V^A(\mathbf{r}) | \psi_i^A \rangle \qquad (10)$$

$$L_a^A = Z_a^A V^A(\mathbf{R}_a^A) \qquad (11)$$

The second, L2, approximation in the X-Pol method is concerned with the numerical calculation of the two-electron four-index integrals of eq 10. In principle, they can be enumerated analytically in exactly the same way as in solving the HF or KS equations,[4] which requires no approximation at this level of the X-Pol hierarchy. However, the enormous amount of such integrals between fragment pairs for a solvated protein present a serious limitation in computational efficiency, a crucial feature required in a force field. Fortunately, extensive investigations of the electrostatic potential of eq 9 using electronic structure methods show that it can be accurately and efficiently determined by a variety of approximate approaches.[41−43] Thus, eq 10 can be determined by a multipole expansion of the two-electron integrals,[44] or transformed into one-electron integrals using an effective ESP that best reproduces the exact results from the electronic structure theory. Such an effective ESP can be expressed in terms multipoles located either on a single center of the fragment or on individual atoms, or in terms of atom-centered partial charges (monopoles).[33,45] Thus, depending on the user's flavor, a series of X-Pol potentials can be developed on the basis of the specific choice of representing the ESP in eq 9.

We choose to use atom-centered monopoles, i.e., partial charges, in the present study to represent the ESP in eq 9.[1−6] Still, there are further considerations to be made. The partial atomic charges can be derived directly from population analysis of the molecular wave function for each fragment, such as the Mulliken population[46] and Lowdin population method. The advantage of using population analysis is that analytical derivatives can be easily computed. The natural orbital technique and the class IV charge models (CM4) are alternative selections.[47] A popular approach, used in classical force field development, which in principle yields the closest agreement with the original ESP, is the ESP-fitted partial charges.[41,42,48] However, it poses difficulty to derive expression for analytical gradient (note that we do not use ESP-fitted charges to compute the Coulomb energy and forces as a substitute for electronic structure calculations as is done in some QM/MM calculations). In this and previous work, we have used the Mulliken charges to approximate the potential defined in eq 9. Recently, Raghavachari and co-workers developed a QM/QM electronic embedding approach using Mulliken popularion charges within the ONIOM framework.[49,50]

The Mulliken population charges for atoms in fragment A are given as follows:

$$q_a^A(\mathbf{R}_a^A) = Z_a^A - \sum_{\mu \in a} (\mathbf{PS})_{\mu\mu} \qquad (12)$$

where $\mathbf{P}$ and $\mathbf{S}$ are standard density and overlap matrices. To best reproduce the ESP in eq 9, we introduce a parameter,[1,2] for neutral fragments only, associated with the second approximation in the X-Pol method to scale the Mulliken charges such that it minimizes the difference in ESP between the electronic structure theory and the monopole representation:

$$\min \left\{ \left| V_{qm}^A(\mathbf{r}) - \lambda \sum_a \frac{q_a^A}{|\mathbf{r} - \mathbf{R}_a^A|} \right| \right\} \qquad (13)$$

This is akin to the ESP-fitting procedure, although there is only one adjustable variable for a given theoretical level and basis set for all neutral molecules here. An alternative interpretation of the parameter λ is that it is optimized to yield the best agreement with experiment for the interaction between two fragments. A more sophisticated scaling scheme may be important when diffuse functions are used to specifically account for charge penetration effects, and this issue has been thoroughly examine in other context.[51,52]

X-Pol Potential

J. Phys. Chem. A, Vol. 113, No. 43, 2009 **11659**

Having defined the partial atomic charges, we write the electrostatic potential at fragment A as

$$V^A(\mathbf{r}) = \sum_{B \neq A} \lambda \left[\sum_b \frac{q_b^B}{|\mathbf{r} - \mathbf{R}_b^B|} \right] \qquad (14)$$

Note that $V_{qm}^A(\mathbf{r})$ in eq 13 is the ESP of molecule A, whereas $V^A(\mathbf{r})$ is the ESP on A due to other fragments. It is interesting to point out that inclusion of eq 14 in the Fock matrix to optimize the wave function and determine the energy of the system is identical to carrying out a total of N combined QM/MM calculations,[53] one for each fragment.

In the present study, we found that it is not necessary to scale the Mulliken population charge at the ab initio Hartree–Fock and DFT level of theory using the 6-31G(d) basis set. It is known that HF/6-31G(d) tends to yield slightly overpolarized atomic charges, almost perfectly mimicking the average polarization effects in aqueous solution.[42] Thus, it is not surprising that for the present set of simple bimolecular complexes, a value of unity is adequate for λ. However, in general, especially when semiempirical quantum models are used, λ ought to be optimized to best reproduce the target experimental data.

2.3. Level-3 (L3) Approximation and Parameterization of the X-Pol Force Field. At this point the X-Pol potential is a fully quantum chemical model such that each molecule or a group of molecules (fragments) is explicitly represented and treated by electronic structure theory, and its interactions with the rest of the system consist of Coulomb (Eint A) and exchange-repulsion and dispersion terms ($E_{int,ed}^A$). Clearly, it would be ideal to use the most accurate electronic structure method along with a large basis set to describe each QM fragment; unfortunately, this would not be feasible, nor is it practical for molecular dynamics simulations of biomolecular systems. Thus, to develop the X-Pol potential into a force field, one must consider two important factors: (1) computational efficiency and (2) the capability for empirical parametrization.[1,2] The first factor is obvious, but the latter may not be so obvious, which may even be counterintuitive because an ab initio theory, albeit with the approximate treatment of interfragment interactions, is brought down to a "semiempirical" level (to be parametrized). Nevertheless, the essence to strive for success of the Lifson-style force fields in biomolecular simulation is the possibility of careful parametrization of potential energy functions against experimental data.[7,15,17,18]

To this end, we have used the formalisms based on the neglect diatomic differential overlap (NDDO)[54] approximation along with the Dewar–Thiel multipole treatment of two-electron integrals for force field developments.[44] The present study, however, focuses on ab initio WFT and DFT, which will eventually be combined with the NDDO X-Pol force field[2,3,6] in a multilayer representation. Thus, the L3 approximation (for the formalism and parametrization of the Coulomb integrals between fragments) in the X-Pol method only concerns the use of Mulliken charges and the $E_{int,ed}^{AB}$ terms in this study.

For the exchange-repulsion and dispersion interaction between different fragments, although it is desirable to employ a general approach that treat the dependence of the $E_{int,ed}^{AB}[\rho^A, \rho^B, \{\zeta^{AB}\}]$ energy on fragment densities explicitly,[55] which will be considered in future work, to proceed, we use the Lennard-Jones potential to parametrically model these effects.[1,3]

$$E_{int,ed}^{AB} \approx \sum_a^A \sum_b^B 4\varepsilon_{ab}^{AB} \left[\left(\frac{\sigma_{ab}^{AB}}{R_{ab}} \right)^{12} - \left(\frac{\sigma_{ab}^{AB}}{R_{ab}} \right)^6 \right] \qquad (15)$$

where the parameters $\{\zeta^{AB} \equiv \varepsilon_{ab}^{AB}, \sigma_{ab}^{AB}\}$ are obtained by standard combining rules from the corresponding atomic parameters such that $\varepsilon_{ab}^{AB} = (\varepsilon_a^A \varepsilon_b^B)^{1/2}$ and $\sigma_{ab}^{AB} = (\sigma_a^A \sigma_b^B)^{1/2}$.

2.4. Double Self-Consistent-Field (DSCF) and the Variational X-Pol Method. There are two ways of optimizing the wave function in eq 1, depending on the way the Fock matrices are constructed. First, if one considers each fragment as an isolated molecule embedded in the environment of the partial charges of the rest of the system, i.e., treating each fragment by the traditional QM/MM approach,[53] the Fock matrix for each fragment can be written as follows:[1–3]

$$\mathbf{F}_{HF,DSCF}^A = \mathbf{H}^A + \sum_i (2\mathbf{J}_i^A - \mathbf{K}_i^A) + \mathbf{I}^A \qquad (16)$$

where $\mathbf{H}^A$ is the one-electron Hamiltonian matrix, $\mathbf{J}_i^A$ and $\mathbf{K}_i^A$ are the Coulomb and exchange integral matrices, and the last term $\mathbf{I}^A$ is the one-electron integral matrix due to the potential given in eq 14. The corresponding KS matrices are given as follows by replacing the exchange integral with the exchange-correlation potential, $v_{xc}^A(\mathbf{r})$:

$$\mathbf{F}_{KS,DSCF}^A = \mathbf{H}^A + \sum_i 2\mathbf{J}_i^A + \sum_i \mathbf{V}_i^A + \mathbf{I}^A \qquad (17)$$

where

$$\mathbf{V}_i^A = \int v_{xc}^A(\mathbf{r}) |\psi_i^A(\mathbf{r})|^2 \, d\mathbf{r} \qquad (18)$$

The total electronic energy of the system can be determined by a double self-consistent-field (DSCF) procedure.[1–3,5] Starting with an initial guess of the one-electron density matrix for each fragment, one loops over all fragments in the system and performs SCF optimization of the orbitals $\{\psi_i^A; i = 1,..., m^A\}$ for each fragment in the presence of the Mulliken charges of all other fragments. This is repeated until the change in total electronic energy or in electron density satisfies a predefined tolerance. The DSCF optimization procedure is straightforward and was the approach proposed in ref 1 and adopted in several subsequently implementations.[29,31] However, a major short coming of the DSCF approach is that the Fock matrix in eq 16 was not derived variationally with respect to a perturbation of the charge density on the total energy (eq 4). Although the total energy obtained by using the DSCF method has negligible deviation from the true minimum energy of the system, it imposes severe difficulty to obtain analytical gradients and one has to make use of the coupled-perturbed Hartree–Fock method to determine forces iteratively.

Alternatively, a set of variational equations for the X-Pol potential has been derived[5] in a way similar to that used by Roothaan in deriving the Hartree–Fock equations. The Fock matrix for the variational X-Pol energy has two additional terms compared with eq 16, resulting from the variation of Mulliken population charges (eq 12):

$$\mathbf{F}^A_{\text{HF,Var}} = \mathbf{H}^A + \sum_i (2\mathbf{J}^A_i - \mathbf{K}^A_i) + \frac{1}{2}\mathbf{I}^A -$$

$$\frac{1}{2}\sum_{B \neq A} \left(\sum_{pq} P^B_{pq} I^{0,B}_{pq} + \sum_{b \in B} L^{0,B}_b \right) \sum_{a \in A}^{\text{on } a} \sum_{\mu}^{\text{in } A} \sum_{\eta} S^A_{\mu\eta} \mathbf{T}^{(\eta,\mu)} \quad (19)$$

where the two terms in parentheses specify the interactions between electron *one* in fragment *A* and the charge densities and nuclear charges of fragment *B*, and the superscript "0" denotes that the matrix element is calculated by setting the charges on atom *a* in fragment *A* to +e (note that the Fock matrix will be multiplied by the density matrix in energy calculation).[5] $\mathbf{T}^{(\eta,\mu)}$ represents a matrix of delta functions for convenience in writing eq 19, and it has been fully described in ref 5. It is matrix element is defined by

$$T^{(\eta,\mu)}_{pq} = \delta_{p\eta}\delta_{\mu q} \quad (20)$$

where $\delta_{p\eta}$ and $\delta_{\mu q}$ are Kronecker deltas. It is interesting to notice that each fragment is fully polarized by the rest of the system, but half of the polarization comes from the Mulliken charges specified by the one-electron integral matrix $\mathbf{I}^A$, and the other half originates from the explicit charge density and nuclear charges in all other fragments.

The corresponding variational KS matrix for the X-Pol potential is

$$\mathbf{F}^A_{\text{DFT,Var}} = \mathbf{H}^A + \sum_i 2\mathbf{J}^A_i + \sum_i \mathbf{V}^A_i + \frac{1}{2}\mathbf{I}^A -$$

$$\frac{1}{2}\sum_{B \neq A} \left(\sum_{pq} P^B_{pq} I^{0,B}_{pq} + \sum_{b \in B} L^{0,B}_b \right) \sum_{a \in A}^{\text{on } a} \sum_{\mu}^{\text{in } A} \sum_{\eta} \lambda S^A_{\mu\eta} \mathbf{T}^{(\eta,\mu)} \quad (21)$$

Obviously, the DSCF optimization procedure can also be applied to eqs 19 and 21 for ab initio HF theory and DFT in the X-Pol potential. Nevertheless, we use the subscript DSCF (eqs 16 and 17) and Var (eqs 19 and 21) to indicate that the first approach is nonvariational and the latter is variational. In practice, it is more efficient to optimize all orbital coefficients simultaneously at each system-SCF iteration. There are also other uses of frozen or constrained fragmental electron density in DFT calculations; here we present a variational approach in which analytical gradient consistent with the potential energy can be obtained for dynamics simulations.

3. Computational Details

The computational procedure of the present X-Pol potential using ab initio HF theory and KS-DFT is identical to the algorithm described previously using a semiempirical NDDO method.[1-5] To illustrate the performance of the ab initio HF and DFT X-Pol method, we optimized hydrogen bonding interactions for a series of bimolecular complexes between water and small organic compounds at the HF and B3LYP levels of theory using the 6-31G(d) basis sets. The computed hydrogen bond geometries and interaction energies are compared with those obtained at the same level of theory by treating the entire system uniformly, and with results obtained using coupled cluster theory at CCSD(T)/aug-cc-pVDZ//B3LYP/aug-cc-pVDZ. We decided not to optimize the geometries at the CCSD(T) level because DFT calculations generally yield excellent geometrical parameters and we do not expect noticeable differences would result from WFT optimizations. The charge scaling parameter

TABLE 1: Lennard-Jones Parameters Used in the X-Pol Potential with B3LYP and the 6-31G(d) Basis Set

atom	σ (Å)	ε (kcal/mol)
H	1.30	0.05
C	3.65	0.15
N	3.45	0.20
O (sp^3)	3.35	0.15
O (sp^2)	3.10	0.15
Cl^-	4.25	0.21
Na^+	2.35	0.30

λ in eq 14 was set to unity, i.e., without any modification of the Mulliken charges in the present ab initio HF and DFT treatment. The initial Lennard-Jones parameters were taken from those optimized for combined QM/MM calculations using the ab initio HF/3-21G method for QM and the OPLS potential[56] for MM,[57] and were slightly adjusted to be adopted in the X-Pol potential. The final parameters are listed in Table 1.

In each bimolecular complex, the monomer geometries are held fixed at the B3LYP optimized structure in X-Pol calculations. Thus, only the hydrogen bond length and angle are optimized. This procedure has been used in the development of the OPLS force field when bimolecular complexes are examined,[56,58] and it has also been used to generate a set of universal parameters in combined QM/MM calculations.[53,57,59]

In the following, we use the short-hand notation XP to specify calculations carried out using the X-Pol potential, followed by "@" to indicate the specific method with which X-Pol calculations are made. Thus, the notation XP@HF/6-31G(d)//B3LYP/6-31G(d) specifies an X-Pol calculation at the HF/6-31G(d) level of theory using the geometry optimized with B3LYP/6-31G(d). All calculations were performed using a locally modified version of the GAMESS package.[60]

4. Results and Discussion

The main goal of this article is to show that the X-Pol method can be conveniently developed to yield excellent results on intermolecular interactions at the ab initio HF and DFT levels of theory with a modest basis set in comparison with experimental and high level ab initio results. We first briefly describe the parametrization philosophy of the X-Pol potential, and present the potential energy profile for a water dimer complex. Then, we consider the results for a set of 14 bimolecular complexes of simple organic molecules with water.

4.1. Parametrization of Repulsive and Dispersive Interactions between Fragments. The approximation to write the total molecular wave function as a Hartree product of the antisymmetric wave functions of individual molecules tremendously reduces computational costs for large systems, which also enables the X-Pol potential to be conveniently parallelized in practical implementations. However, this is at the expense of neglecting short-range exchange repulsions and long-range dispersion attractions between different fragments. Thus, to retain the computational accuracy of the entire system that is treated as one fragment, one must introduce a formalism to remedy this difference. To this end, we have decided to use a purely empirical approach, making use of the Lennard-Jones potential to parametrically model the repulsive and dispersive interactions. Furthermore, it provides an opportunity to parametrize the X-Pol potential to yield results for intermolecular interactions in better agreement with experiment with the use of a modest level of electronic structure method.

Table 1 lists a set of Lennard-Jones parameters used in the present calculation, which were adjusted for the XP@B3LYP/
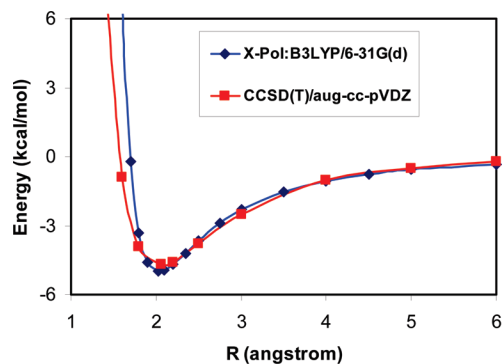
X-Pol Potential

J. Phys. Chem. A, Vol. 113, No. 43, 2009 **11661**

Figure 1. Interaction energy profile of water dimer as a function of the hydrogen bond distance from CCSD(T)/aug-cc-pVDZ (red) and XP@B3LYP/6-31G(d) optimizations.

6-31G(d) model, starting with those optimized in combined QM/MM calculations at the HF/3-21G level,[57] to reproduce the results for 14 bimolecular complexes obtained from CCSD(T)/aug-cc-pVDZ//B3LYP/aug-cc-pVDZ. There is no attempt made here in choosing a training set and a test set of complexes for validation, but a thorough comparison will be made in a later publication. As it turns out, the X-Pol parameters are very similar to those of the ab initio QM/MM values. These parameters were employed in the XP@HF/6-31G(d) calculations without further alteration, although in principle a different set of parameters may be needed for different methods and basis functions. The aim of the present study is not to provide a set of optimized parameters for the X-Pol potential; we aim to illustrate that a set of atomistic parameters can yield excellent results for bimolecular interactions using the X-Pol potential, in better agreement with high level ab initio data than the full B3LYP/6-31G(d) and HF/6-31G(d) results.

4.2. Potential Profile for the Water Dimer. In Figure 1, we first examine the potential energy profile of the water dimer as a function of the hydrogen-bond distance using XP@B3LYP/6-31G(d) compared with that fully optimized at the CCSD(T)/aug-cc-pVDZ level. The computed interaction energy is 5.0 kcal/mol from the X-Pol potential, which is in good agreement with a value of 4.8 kcal/mol using CCSD(T). The corresponding hydrogen bond distances are, respectively, 1.98 and 1.96 Å, also in excellent accord. At short distance, the repulsive interactions increase more quickly than that of the CCSD(T) curve, indicating that a softer repulsive potential than that of the Lennard-Jones potential may be more appropriate. The attractive part of the potential profile is in excellent agreement between the XP@B3LYP and CCSD(T) calculations. Notice that the full B3LYP/6-31G(d) calculations overestimate the binding energy for the water dimer, whereas increasing the size of the basis function to aug-cc-pVDZ improves its agreement with high-level ab initio results (Table 2). The good performance of the X-Pol potential for bimolecular interactions is due to its capability to empirically adjust the repulsive and dispersive interactions. In a recent study, Fujimoto and Yang described a frozen-fragment interaction calculation,[61] in which the KS orbitals are polarized by the charge densities of other fragments similar to the method described here.[1-3] However, using B3LYP/6-31G(d), these authors reported an error of −33.1 kcal/mol for the water dimer over the full QM result at the same level of theory, which overestimates the interaction energy only by 2 kcal/mol than that from CCSD(T)/aug-cc-pVDZ. Thus, the net error from that implementation is more than 35 kcal/mol for $(H_2O)_2$, emphasizing the significance of an adequate treatment of the repulsive and attractive interactions.

4.3. Bimolecular Complexes. We considered nine bimolecular complexes of water with water, methanol, formamide, and immidazole (Table 2), and five ion−water complexes from chloride, sodium, and acetate ions (Table 3) to illustrate the feasibility that the X-Pol potential implemented with ab initio HF and DFT approaches can yield adequate description of intermolecular interactions. Furthermore, we do not aim to simply reproduce the interaction energies of the corresponding HF/6-31G(d) or B3LYP/6-31G(d) data, the same levels of theory used in the X-Pol calculations, because the latter in fact has significantly large errors in comparison with CCSD(T) results. When larger basis functions are used, the B3LYP results improve considerably, but the use of a very large basis set is not desirable in the present X-Pol model for treating large systems including protein and nucleic acids. On the other hand, with an adjustment of the van der Waals parameters (Table 1), we found that it is possible to obtain good agreement between X-Pol and CCSD(T) calculations with a reasonable, but with the use of a modest basis set in X-Pol calculations.

The CCSD(T) interaction energy fully optimized using the aug-cc-pVDZ basis set for the water dimer is 4.9 kcal/mol (Figure 1), which is in excellent agreement with the experimental value of 4.9 ± 0.9 kcal/mol determined from pressure broadening of near-IR spectra.[62,63] The results listed in Table 2 were obtained by partial geometry optimizations with the monomer geometry fixed,[56-59] and the corresponding CCSD(T) interaction energies were computed by single point calculations using the B3LYP/aug-cc-pVDZ geometries. Thus, the dimer interaction energy for water is slightly greater than that from full CCSD(T) optimizations. The computed interaction energies are 5.0 kcal/mol from both XP@HF/6-31G(d) and XP@B3LYP/6-31G(d) optimizations. For the methanol−water bimolecular complex, there are two possible hydrogen bonding interactions, depending on water or methanol as the hydrogen bond donor. The XP@B3LYP model yields interaction energies of 5.2 and 4.8 kcal/mol, in favor of the complex in which water acts as the hydrogen bond donor. The same trend is reproduced for the full QM system at the CCSD(T) and B3LYP/aug-cc-pVDZ levels, whereas B3LYP/6-31G(d) optimizations yielded the opposite trend. An early study of the methanol−water system by Krischner and Woods yielded interaction energies of −5.7 and −4.9 kcal/mol using MP2/aug-cc-pVQZ//MP2/aug-cc-pVTZ,[64] in accord with the present X-Pol results.

For the immidazole−water complexes, we found that the immizaole ring is a better hydrogen bond acceptor from water than donating a hydrogen bond using the X-Pol potential. This is in agreement with high-level ab initio results in Table 2, although the difference is greater using CCSD(T) calculations. Again, B3LYP/6-31G(d) yields the opposite trend, suggesting that a much larger basis set than 6-31G(d) is needed in studies of enzymes. Four structures were considered in the formamide−water complex. In accord with experiment,[65] the structure with a water simultaneously donating a hydrogen bond to the carbonyl group and accepting one from the amide group is the global minimum. The computed XP@B3LYP/6-31G(d) interaction energy of −7.6 kcal/mol is in good accord with the CCSD(T) results. Overall, the carbonyl group forms strong hydrogen bonds with water than the amide unit donating hydrogen bonds to water.[66]

The interaction energies for chloride ion and sodium ion with water can be fitted exactly to the CCSD(T) or experimental results, the latter of which are −14.8 and +24 kcal/mol experimentally.[67,68] The ab initio results are slightly smaller, noting that the experimental values are enthalpies of interaction.
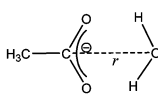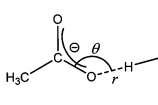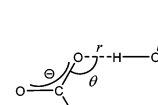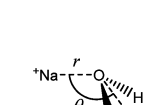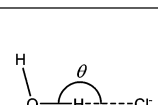
TABLE 2: Computed Geometries and Interaction Energies for Molecule−Water Bimolecular Complexes

Complex	Method	r (Å)	θ (degrees)	ΔE (kcal/mol)
	HF/6-31G(d)	2.03	129.3	-5.6
	B3LYP/6-31G(d)	1.93	109.1	-7.5
	B3LYP/aug-cc-pVDZ	1.95	129.8	-4.6
	CCSD(T)/aug-cc-pVDZ			-5.2
	XP@HF/6-31G(d)	1.99	145.0	-5.0
	XP@B3LYP/6-31G(d)	2.03	144.0	-5.0
	HF/6-31G(d)	2.02	132.1	-5.5
	B3LYP/6-31G(d)	1.91	112.2	-7.5
	B3LYP/aug-cc-pVDZ	1.96	130.0	-4.4
	CCSD(T)/aug-cc-pVDZ			-5.4
	XP@HF/6-31G(d)	2.01	123.0	-4.3
	XP@B3LYP/6-31G(d)	2.05	150.5	-4.8
	HF/6-31G(d)	2.02	130.4	-5.5
	B3LYP/6-31G(d)	1.91	118.9	-7.0
	B3LYP/aug-cc-pVDZ	1.92	134.9	-5.0
	CCSD(T)/aug-cc-pVDZ			-5.9
	XP@HF/6-31G(d)	1.98	130.0	-5.4
	XP@B3LYP/6-31G(d)	2.03	135.5	-5.2
	HF/6-31G(d)	2.12	115.8	-6.4
	B3LYP/6-31G(d)	2.01	117.9	-7.1
	B3LYP/aug-cc-pVDZ	1.96	120.1	-6.6
	CCSD(T)/aug-cc-pVDZ			-7.5
	XP@HF/6-31G(d)	1.97	117.0	-6.6
	XP@B3LYP/6-31G(d)	2.02	117.0	-6.9
	HF/6-31G(d)	2.04	202.7	-6.3
	B3LYP/6-31G(d)	1.93	132.9	-7.9
	B3LYP/aug-cc-pVDZ	1.99	170.5	-5.4
	CCSD(T)/aug-cc-pVDZ			-6.6
	XP@HF/6-31G(d)	1.97	180.0	-5.6
	XP@B3LYP/6-31G(d)	2.00	178.5	-6.6
	HF/6-31G(d)	2.02	116.8	-6.2
	B3LYP/6-31G(d)	1.93	112.1	-7.3
	B3LYP/aug-cc-pVDZ	1.91	116.2	-5.8
	CCSD(T)/aug-cc-pVDZ			-6.4
	XP@HF/6-31G(d)	1.85	125.0	-6.6
	XP@B3LYP/6-31G(d)	1.92	123.5	-6.3
	HF/6-31G(d)	1.98	111.8	-7.2
	B3LYP/6-31G(d)	1.88	104.8	-9.2
	B3LYP/aug-cc-pVDZ	1.86	110.4	-6.7
	CCSD(T)/aug-cc-pVDZ			-7.6
	XP@HF/6-31G(d)	1.84	110.0	-8.2
	XP@B3LYP/6-31G(d)	1.89	113.0	-7.6
	HF/6-31G(d)	2.09	111.9	-5.9
	B3LYP/6-31G(d)	1.97	103.1	-8.2
	B3LYP/aug-cc-pVDZ	2.04	115.0	-5.0
	CCSD(T)/aug-cc-pVDZ			-6.0
	XP@HF/6-31G(d)	1.99	146.0	-4.9
	XP@B3LYP/6-31G(d)	2.02	127.5	-5.7
	HF/6-31G(d)	2.09	181.4	-5.6
	B3LYP/6-31G(d)	1.97	130.2	-7.1
	B3LYP/aug-cc-pVDZ	2.04	167.7	-4.7
	CCSD(T)/aug-cc-pVDZ			-5.7
	XP@HF/6-31G(d)	2.00	183.0	-5.4
	XP@B3LYP/6-31G(d)	2.03	176.5	-5.9

Using the parameters in Table 1, the X-Pol interaction energies for these two ions with water are, respectively, −14.1 and −22.9 kcal/mol, in reasonable accord with the CCSD(T) results (Table 3). The most stable complex between acetate ion and water is the bidentate structure in which both hydrogen atoms of water donate hydrogen bonds to the two oxygen atoms of acetate ion. The interaction energy from CCSD(T) calculation is −18.3 kcal/mol, slightly stronger than the single-hydrogen bonded complex in the syn orientation (−18.0 kcal/mol) (Table 3).[58,67,69] The corresponding X-Pol results are −18.3 and −18.2 kcal/mol using the XP@B3LYP/6-31G(d) and are −18.9 and −18.4 from XP@HF/6-31G(d). The hydrogen-bond complex from the anti orientation is the least stable, with computed interaction energies of −16.2, −15.9, and −16.4 kcal/mol from CCSD(T),

X-Pol Potential

J. Phys. Chem. A, Vol. 113, No. 43, 2009 **11663**

TABLE 3: Computed Geometries and Interaction Energies for Ion−Water Complexes

Complex	Method	r (Å)	θ (degrees)	ΔE (kcal/mol)
	HF/6-31G(d)	3.26		-18.4
	B3LYP/6-31G(d)	3.12		-24.2
	B3LYP/aug-cc-pVDZ	3.16		-17.1
	CCSD(T)/aug-cc-pVDZ			-18.3
	XP@HF/6-31G(d)	3.15		-18.9
	XP@B3LYP/6-31G(d)	3.19		-18.3
	HF/6-31G(d)	1.88	102.3	-19.4
	B3LYP/6-31G(d)	1.80	101.3	-22.8
	B3LYP/aug-cc-pVDZ	1.76	110.0	-17.0
	CCSD(T)/aug-cc-pVDZ			-18.0
	XP@HF/6-31G(d)	1.78	106.0	-18.4
	XP@B3LYP/6-31G(d)	1.82	104.0	-18.2
	HF/6-31G(d)	1.82	130.0	-15.1
	B3LYP/6-31G(d)	1.74	123.0	-19.1
	B3LYP/aug-cc-pVDZ	1.71	127.9	-15.3
	CCSD(T)/aug-cc-pVDZ			-16.2
	XP@HF/6-31G(d)	1.73	134.0	-16.4
	XP@B3LYP/6-31G(d)	1.76	136.5	-15.9
	HF/6-31G(d)	2.21	179.9	-28.6
	B3LYP/6-31G(d)	1.19	180.0	-31.0
	B3LYP/aug-cc-pVDZ	2.21	179.9	-23.9
	CCSD(T)/aug-cc-pVDZ			-22.0
	XP@HF/6-31G(d)	2.38	180.0	-24.3
	XP@B3LYP/6-31G(d)	2.40	174.0	-22.9
	HF/6-31G(d)	2.38	157.8	-13.9
	B3LYP/6-31G(d)	2.23	161.7	-16.7
	B3LYP/aug-cc-pVDZ	2.19	168.8	-13.8
	CCSD(T)/aug-cc-pVDZ			-14.1
	XP@HF/6-31G(d)	2.32	160.5	-14.7
	XP@B3LYP/6-31G(d)	2.33	164.0	-14.1

XP@B3LYP, and XP@HF calculations. The experimental enthalpy of binding is about −16 kcal/mol and argues against the bidentate complex in the gas phase.[67]

The mean unsigned error from CCSD(T) results for the fourteen complexes considered is 0.4 kcal/mol for the XP@B3LYP/6-31G(d) method (Figure 2), whereas it is 0.9 kcal/mol from the XP@HF/6-31G(d) potential, a reflection that the Lennard-Jones parameters were not optimized for HF calculations in Table 1. In both cases, we have used the monomer structures optimized at the B3LYP/6-31G(d) level. Hydrogen bond distances from optimizations using XP@B3LYP/6-31G(d) are in good accord with those obtained from B3LYP/aug-cc-

pVDZ calculations. The mean unsigned error for the fourteen complexes considered is 0.08 Å. This is comparable to ab initio QM/MM calculations for similar bimolecular complexes.[57] The good agreement suggests that the X-Pol potential can be trained by introducing a set of atomistic parameters, associated with a given theory and basis function, to yield adequate results for the description of intermolecular interactions that are approximated by a Hartree product wave function.

5. Concluding Remarks

The explicit polarization (X-Pol) method was developed as a framework to develop next-generation force fields for biomolecular simulations based on electronic structure theory, and it has been demonstrated to be feasible for extended molecular dynamics simulation of a solvated protein. Importantly the X-Pol method is a general theory, which can be employed with any level of electronic structure theory. In principle, it is possible and desirable to treat the central region of interest by a high-level ab initio method or density functional theory and the remainder of the system is represented by an NDDO-type X-Pol force field. The present study examines the X-Pol approach using ab initio molecular orbital theory at the Hartree−Fock level and density functional theory using a hybrid functional. The computational results are illustrated by considering a set of bimolecular complexes of small organic molecules and ions with water. The computed interaction energies and hydrogen bond geometries are in good accord with CCSD(T) results and B3LYP/aug-cc-pVDZ optimizations.

The X-Pol potential complements the effective fragment potential (EFP) approach developed by Gordon and co-workers
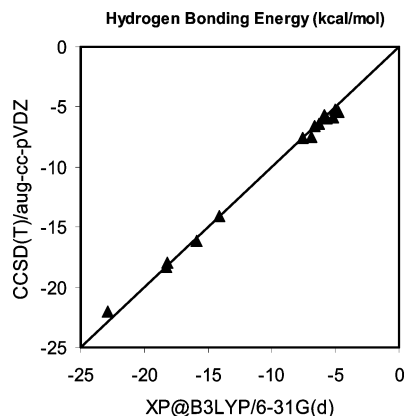

Figure 2. Comparison of the computed interaction distances for bimolecular complexes optimized using B3LYP/aug-cc-pVDZ and XP@B3LYP/6-31G(d) methods.

11664 *J. Phys. Chem. A, Vol. 113, No. 43, 2009*

Song et al.

using ab initio MO theory and DFT. The main difference is that the electronic structure for each individual fragment is fully optimized under the electric field of the rest of the system for a given instantaneous geometrical configuration in the X-Pol, whereas the EFP is determined from a set of distributed multipole expansions to account for static and polarization interactions as well as charge penetration and transfer. The significance of and methods developed to treat charge penetration in the EFP model can be adopted for X-Pol calculations. On the other hand, the X-Pol potential can be designed as a force field parametrized to reproduce experimental liquid properties, and a combination of such an X-Pol force field and ab initio X-Pol treatment represents a general multilayer quantum mechanical approach for biomolecular systems.

References and Notes

(1) Gao, J. *J. Phys. Chem. B* **1997**, *101*, 657–663.
(2) Gao, J. *J. Chem. Phys.* **1998**, *109*, 2346–2354.
(3) Xie, W.; Gao, J. *J. Chem. Theory Comput.* **2007**, *3*, 1890–1900.
(4) Xie, W.; Song, L.; Truhlar, D. G.; Gao, J. *J. Phys. Chem. B* **2008**, *112*, 14124–14131.
(5) Xie, W.; Song, L.; Truhlar, D. G.; Gao, J. *J. Chem. Phys.* **2008**, *128*, 234108/234101–234109.
(6) Xie, W.; Orozco, M.; Truhlar, D. G.; Gao, J. *J. Chem. Theory Comput.* **2009**, *5*, 459–467.
(7) Bixon, M.; Lifson, S. *Tetrahedron* **1967**, *23*, 769–784.
(8) Levitt, M. *Nat. Struct. Biol.* **2001**, *8*, 392–393.
(9) Hill, T. L. *J. Chem. Phys.* **1946**, *14*, 465.
(10) Westheimer, F. H.; Mayer, J. E. *J. Chem. Phys.* **1946**, *14*, 733–738.
(11) Hendrickson, J. B. *J. Am. Chem. Soc.* **1961**, *83*, 4537–4547.
(12) Burkert, U.; Allinger, N. L. *Molecular Mechanics*; American Chemical Society: Washington, D.C., 1982.
(13) Levitt, M.; Lifson, S. *J. Mol. Biol.* **1969**, *46*, 269–279.
(14) McCammon, J. A.; Gelin, B. R.; Karplus, M. *Nature (London)* **1977**, *267*, 585–590.
(15) For a special issue on the current development of polarizable force field, see Jorgensen, W. L. *J. Chem. Theory Comput.* **2007**, *3*, 1877.
(16) Vesely, F. J. *J. Comput. Phys.* **1977**, *24*, 361–371.
(17) Dinur, U.; Hagler, A. T. *Rev. Comput. Chem.* **1991**, *2*, 99–164.
(18) MacKerell, A. D., Jr. *Ann. Rep. Comput. Chem.* **2005**, *1*, 91–102.
(19) Dewar, M. J. S.; Zoebisch, E. G.; Healy, E. F.; Stewart, J. J. P. *J. Am. Chem. Soc.* **1985**, *107*, 3902–3909.
(20) Wierzchowski, S. J.; Kofke, D. A.; Gao, J. *J. Chem. Phys.* **2003**, *119*, 7365–7371.
(21) Yang, W.; Lee, T.-S. *J. Chem. Phys.* **1995**, *103*, 5674–5678.
(22) Dixon, S. L.; Merz, K. M., Jr. *J. Chem. Phys.* **1997**, *107*, 879–893.
(23) Van Der Vaart, A.; Gogonea, V.; Dixon, S. L.; Merz, K. M., Jr. *J. Comput. Chem.* **2000**, *21*, 1494–1504.
(24) Raha, K.; Merz, K. M., Jr. *J. Med. Chem.* **2005**, *48*, 4558–4575.
(25) Stewart, J. J. P. *Int. J. Quantum Chem.* **1996**, *58*, 133–146.
(26) Gao, J. *J. Comput. Chem.* **1997**, *18*, 1062–1971.
(27) Thompson, M. A. *J. Phys. Chem.* **1996**, *100*, 14492–14507.
(28) Kitaura, K.; Sawai, T.; Asada, T.; Nakano, T.; Uebayasi, M. *Chem. Phys. Lett.* **1999**, *312*, 319–324.
(29) Kitaura, K.; Ikeo, E.; Asada, T.; Nakano, T.; Uebayasi, M. *Chem. Phys. Lett.* **1999**, *313*, 701–706.

(30) Fukuzawa, K.; Mochizuki, Y.; Tanaka, S.; Kitaura, K.; Nakano, T. *J. Phys. Chem. B* **2006**, *110*, 16102–16110.
(31) Gascon, J. A.; Leung, S. S. F.; Batista, E. R.; Batista, V. S. *J. Chem. Theory Comput.* **2006**, *2*, 175–186.
(32) Field, M. J. *Mol. Phys.* **1997**, *91*, 835–845.
(33) Day, P. N.; Jensen, J. H.; Gordon, M. S.; Webb, S. P.; Stevens, W. J.; Krauss, M.; Garmer, D.; Basch, H.; Cohen, D. *J. Chem. Phys.* **1996**, *105*, 1968–1986.
(34) Gordon, M. S.; Slipchenko, L.; Li, H.; Jensen, J. H. *Ann. Rep. Comput. Chem.* **2007**, *3*, 177–193.
(35) Gao, J.; Amara, P.; Alhambra, C.; Field, M. J. *J. Phys. Chem. A* **1998**, *102*, 4714–4721.
(36) Amara, P.; Field, M. J.; Alhambra, C.; Gao, J. *Theor. Chem. Acc.* **2000**, *104*, 336–343.
(37) Pu, J.; Gao, J.; Truhlar, D. G. *J. Phys. Chem. A* **2004**, *108*, 5454–5463.
(38) Pu, J.; Gao, J.; Truhlar, D. G. *J. Phys. Chem. A* **2004**, *108*, 632–650.
(39) Pu, J.; Gao, J.; Truhlar, D. G. *ChemPhysChem* **2005**, *6*, 1853–1865.
(40) Kohn, W.; Becke, A. D.; Parr, R. G. *J. Phys. Chem.* **1996**, *100*, 12974–12980.
(41) Momany, F. A. *J. Phys. Cem.* **1978**, *82*, 592–601.
(42) Wang, J.; Cieplak, P.; Kollman, P. A. *J. Comput. Chem.* **2000**, *21*, 1049–1074.
(43) Alhambra, C.; Luque, E. J.; Orozco, M. *J. Comput. Chem.* **1994**, *15*, 12–22.
(44) Dewar, M. J. S.; Thiel, W. *Theoret. Chim. Acta* **1977**, *46*, 89–104.
(45) Stone, A. J. *Chem. Phys. Lett.* **1981**, *83*, 233–239.
(46) Mulliken, R. S. *J. Chem. Phys.* **1964**, *61*, 20.
(47) Li, J.; Zhu, T.; Cramer, C. J.; Truhlar, D. G. *J. Phys. Chem. A* **2000**, *104*, 2178–2182.
(48) Gao, J.; Luque, F. J.; Orozco, M. *J. Chem. Phys.* **1993**, *98*, 2975–2982.
(49) Hratchian, H. P.; Parandekar, P. V.; Raghavachari, K.; Frisch, M. J.; Vreven, T. *J. Chem. Phys.* **2008**, *128*, 034107.
(50) Parandekar, P. V.; Hratchian, H. P.; Raghavachari, K. *J. Chem. Phys.* **2008**, *129*, 145101.
(51) Freitag, M. A.; Gordon, M. S.; Jensen, J. H.; Stevens, W. J. *J. Chem. Phys.* **2000**, *112*, 7300–7306.
(52) Stone, A. J. *The Theory of Intermolecular Forces*; Oxford University Press: Oxford, U.K., 1996.
(53) Gao, J.; Xia, X. *Science* **1992**, *258*, 631–635.
(54) Pople, J. A.; Santry, D. P.; Segal, G. A. *J. Chem. Phys.* **1965**, *43*, S129–S135.
(55) Gordon, M. S.; Freitag, M. A.; Bandyopadhyay, P.; Jensen, J. H.; Kairys, V.; Stevens, W. J. *J. Phys. Chem. A* **2001**, *105*, 293–307.
(56) Jorgensen, W. L.; Maxwell, D. S.; Tirado-Rives, J. *J. Am. Chem. Soc.* **1996**, *118*, 11225–11236.
(57) Freindorf, M.; Gao, J. *J. Comput. Chem.* **1996**, *17*, 386–395.
(58) Jorgensen, W. L.; Gao, J. *J. Phys. Chem.* **1986**, *90*, 2174–2182.
(59) Gao, J. *ACS Symp. Ser.* **1994**, *569*, 8–21.
(60) Schmidt, M. W.; Baldridge, K. K.; Boatz, J. A.; Elbert, S. T.; Gordon, M. S.; Jensen, J. H.; Koseki, S.; Matsunaga, N.; Nguyen, K. A.; et al. *J. Comput. Chem.* **1993**, *14*, 1347–1363.
(61) Fujimoto, K.; Yang, W. *J. Chem. Phys.* **2008**, *129*, 054102.
(62) Fiadzomor, P. A. Y.; Keen, A. M.; Grant, R. B.; Orr-Ewing, A. J. *Chem. Phys. Lett.* **2008**, *462*, 188–191.
(63) Nakayama, T.; Fukuda, H.; Kamikawa, T.; Sakamoto, Y.; Sugita, A.; Kawasaki, M.; Amano, T.; Sato, H.; Sakaki, S.; Morino, I.; Inoue, G. *J. Chem. Phys.* **2007**, *127*, 134302.
(64) Kirschner, K. N.; Woods, R. J. *J. Phys. Chem. A* **2001**, *105*, 4150–4155.
(65) Lovas, F. J.; Suenram, R. D.; Fraser, G. T.; Gillies, C. W.; Zozom, J. *J. Chem. Phys.* **1988**, *88*, 722–729.
(66) Bende, A.; Suhai, S. *Int. J. Quantum Chem.* **2005**, *103*, 841–853.
(67) Meot-Ner, M. *J. Am. Chem. Soc.* **1988**, *110*, 3854–3858.
(68) Kebarle, P. *Annu. Rev. Phys. Chem.* **1977**, *28*, 445–476.
(69) Gao, J.; Garner, D. S.; Jorgensen, W. L. *J. Am. Chem. Soc.* **1986**, *108*, 4784–4790.